# 二维配位聚合物$[Tb(1,4\text{-}bdc)_{1.5}(phen)(H_2O)]_n$的合成、晶体结构及对$Fe^{3+}$离子的荧光检测

汪子微[1] 吴浩东[1] Muhammad Yaseen[2] 梁艾琳[1] 刘 贺[1]
宁子昂[1] 王 帅[1] 王 刚[1] 全 葳[1] 王 浩*,[1]
([1]北京石油化工学院新材料与化工学院,特种弹性体复合材料北京市重点实验室,北京 102617)
([2]University of Peshawar, Institute of Chemical Sciences, Peshawar 25120, Pakistan)

**摘要:** 通过溶剂热反应成功合成出一种新型2D配位聚合物$[Tb(1,4\text{-}bdc)_{1.5}(phen)(H_2O)]_n$ (**1**)(1,4-$H_2$bdc=对苯二甲酸;phen=菲咯啉)。对其进行了单晶X射线衍射、粉末X射线衍射、红外光谱、元素分析、荧光光谱表征。X射线衍射晶体学分析表明,配合物**1**结晶于三斜晶系$P\bar{1}$空间群,2个相邻的Tb(Ⅲ)离子与4个1,4-$bdc^{2-}$通过—O—C—O—桥联成双核单元,并进一步通过1,4-$bdc^{2-}$桥联成二维层状结构。荧光实验证明配合物**1**可以通过荧光猝灭机制检测$Fe^{3+}$,$K_{sv}$=8.39×$10^3$ L·$mol^{-1}$,检测限为0.017 μmol·$L^{-1}$。

**关键词:** 配位聚合物;晶体结构;荧光检测
**中图分类号:** O614.341 **文献标识码:** A **文章编号:** 1001-4861(2022)03-0551-08
**DOI:** 10.11862/CJIC.2022.056

## Two-Dimensional Coordination Polymer $[Tb(1,4\text{-}bdc)_{1.5}(phen)(H_2O)]_n$: Synthesis, Crystal Structure and Luminescent Detection of $Fe^{3+}$

WANG Zi-Wei[1] WU Hao-Dong[1] Muhammad Yaseen[2] LIANG Ai-Lin[1] LIU He[1]
NING Zi-Ang[1] WANG Shuai[1] WANG Gang[1] QUAN Wei[1] WANG Hao*,[1]
([1]*Beijing Key Lab of Special Elastomer Composite Materials, College of New Materials and Chemical Engineering, Beijing Institute of Petrochemical Technology, Beijing* 102617, *China*)
([2]*Institute of Chemical Sciences, University of Peshawar, Peshawar* 25120, *Pakistan*)

**Abstract:** Two-dimensional coordination polymer of $[Tb(1,4\text{-}bdc)_{1.5}(phen)(H_2O)]_n$ (**1**) (1,4-$H_2$bdc=terephthalic acid, phen=1,10-phenanthroline) was synthesized by solvothermal approach. Complex **1** was characterized by single-crystal X-ray diffraction, powder X-ray diffraction, FT-IR spectroscopy, elemental analysis, and fluorescence spectra. X-ray diffraction crystallographic analyses show that complex **1** crystallizes in the triclinic crystal system $P\bar{1}$ space group; two adjacent Tb(Ⅲ) ions are bridged by —O—C—O— from four 1,4-$bdc^{2-}$ into a binuclear unit, and further bridged by 1,4-$bdc^{2-}$ into an infinite 2D layered structure. The fluorescence experiment proved that the complex **1** can detect $Fe^{3+}$ through the fluorescence quenching mechanism with $K_{sv}$=8.39×$10^3$ L·$mol^{-1}$ and limit of detection of 0.017 μmol·$L^{-1}$. CCDC: 2095406.

**Keywords:** coordination polymer; crystal structure; luminescence sensing

收稿日期:2021-09-14。收修改稿日期:2021-11-20。
北京市自然科学基金(No.2212006)和"十三五"时期北京市属高校高水平教师队伍建设支持计划(No.CIT&TCD201904044)资助。
*通信联系人。E-mail:wangh@bipt.edu.cn

## 0 Introduction

The uncontrolled release of iron ions into air and water sources leading to several types of environmental pollutions are human health hazards[1-3]. Therefore, it is important to develop a simple and efficient method for the detection of $Fe^{3+}$. Among many reported sensing approaches, fluorescence sensing has received extensive attention attributed to its high sensitivity, low detection limit, and fast detection speed[4-5]. Therefore, a fluorescence sensor can be developed to detect low-concentration of $Fe^{3+}$ [6-9].

Coordination polymers (CPs) are fascinating materials that are both fundamentally important and technologically relevant[10-11] and have been extensively studied, not only because of their diverse structures, but also for their wide application prospects in the fields of molecular storage, luminescence, and magnetism[12-14]. Currently, luminescent coordination polymers (LCPs) as fluorescent probes have become one of the research hotspots, which can effectively monitor the presence of iron ions based on the fluorescence quenching mechanism[15].

The application of the mixed ligands strategy has been proved an effective method to construct a variety of CPs[16-21]. In this work, a new $Tb^{3+}$ CP with terephthalic acid (1, 4 - bdc) and 1, 10 - phenanthroline (phen), $[Tb(1,4\text{-bdc})_{1.5}(phen)(H_2O)]_n$ (**1**), was synthesized and structurally determined using mixed ligands strategy. The resulting CP exhibited high luminescence sensing performance for $Fe^{3+}$ with a fluorescence quenching mechanism.

## 1 Experimental

### 1.1 Reagents and characterization

Terbium nitrate hexahydrate, 1, 10 - phenanthroline, and terephthalic acid were of commercial grade and used without further purification. Powder X - ray diffraction (PXRD) patterns were recorded on a Rigaku D/Max-2500 diffractometer (Cu $K\alpha$, $\lambda$=0.154 06 nm, $2\theta$ =5°-50°, $U$=40 kV, $I$=40 mA), having a graphite monochromator. Simulation of the PXRD pattern was carried out by the single - crystal data and diffraction - crystal module of the Mercury program version 1.4.2. Elemental analyses for C, H, and N were performed on a Perkin-Elemer240C analyzer. FT - IR spectra of the powder samples were collected on a Nicolet IS10 infrared spectrum radiometer in a wavenumber range of 4 000-400 $cm^{-1}$ using the KBr pellets. The luminescence spectra and luminescence lifetimes properties were measured with the FS5 fluorescence spectrometer (Edinburgh Instruments).

### 1.2 Synthesis of the title complex

1,4-$H_2$bdc (8 mg, 0.05 mmol), $Tb(NO_3)_3\cdot 6H_2O$ (21 mg, 0.05 mmol), phen (9 mg, 0.05 mmol) and $H_2O$/DMAC/EtOH (5 mL, 1∶1∶1, $V/V$) were sealed in a clear glass vial (10 mL), heated at 95 ℃ for 72 h, and then cooled slowly to room temperature. The colorless and sticklike crystals were obtained and washed with ethanol with a yield of 20% (based on $Tb^{3+}$). Anal. Calcd. for $C_{24}H_{16}N_2O_7Tb$(%): C, 47.77; H, 2.65; N, 4.64. Found (%): C, 47.81; H, 2.77; N, 4.83. IR (KBr pellet, $cm^{-1}$): 2 819(w), 2 671(w), 2 545(w), 1 678(s), 1 396(s), 1 390(s), 1 387(s), 1 286(s), 1 020(m), 933(m), 781(m), 728(vs).

### 1.3 XRD structural determination

Diffraction data of **1** were collected on a Bruker D8 venture diffractometer with graphite - monochromator at 293(2) K with Mo $K\alpha$ radiation ($\lambda$ =0.071 073 nm). The crystal data was solved by direct methods using the SHELXS-2014 program and refined by full-matrix least-squares methods on $F^2$ using the program SHELXL-2014. Metal atoms in the complex were located from the E - maps while non - hydrogen atoms were located in successive difference Fourier syntheses and refined with anisotropic thermal parameters on $F^2$. Hydrogen atoms of the ligands were generated theoretically onto the specific atoms and refined with fixed thermal factors. The crystallographic data and experimental details for structural analyses are summarized in Table 1. Selected bond lengths for the complex are listed in Table 2.

CCDC: 2095406.

## 2 Results and discussion

### 2.1 Structural description of 1

X-ray single-crystal analysis reveals that complex **1** crystallizes in the triclinic space group $P\bar{1}$. The asym-

**Table 1 Crystallographic data and structural refinements of complex 1**

| Parameter | 1 | Parameter | 1 |
|---|---|---|---|
| Empirical formula | $C_{24}H_{16}N_2O_7Tb$ | $Z$ | 2 |
| Formula weight | 603.31 | $D_c$ / (g·cm$^{-3}$) | 1.835 |
| $\theta$ range / (°) | 2.2-26.5 | $\mu$ / mm$^{-1}$ | 3.29 |
| Crystal system | Triclinic | F(000) | 590 |
| Space group | $P\bar{1}$ | Measured reflection | 19 438 |
| $a$ / nm | 1.028 53(4) | Independent reflection | 6 249 |
| $b$ / nm | 1.081 88(4) | Reflection with $I>2\sigma(I)$ | 5 415 |
| $c$ / nm | 1.132 75(3) | $R_{int}$ | 0.049 |
| $\alpha$ / (°) | 107.375(3) | $R$ [$F^2>2\sigma(F^2)$] | 0.034 |
| $\beta$ / (°) | 91.669(3) | $wR$ ($F^2$) | 0.089 |
| $\gamma$ / (°) | 112.992(4) | Goodness-of-fit (on $F^2$) | 1.07 |
| $V$ / nm$^3$ | 1.092 04(7) | | |

**Table 2 Selected bond lengths (nm) and bond angles (°) of 1**

| | | | | | |
|---|---|---|---|---|---|
| Tb1—O7$^i$ | 0.228 7(3) | Tb1—O6$^i$ | 0.233 0(3) | Tb1—O1 | 0.233 4(3) |
| Tb1—O4 | 0.235 9(3) | Tb1—O3 | 0.237 4(3) | Tb1—O1W | 0.247 5(3) |
| Tb1—N1 | 0.257 4(3) | Tb1—N2 | 0.260 5(4) | | |
| O7$^i$—Tb1—O6$^i$ | 73.30(13) | O7$^i$—Tb1—O1 | 84.33(11) | O6$^i$—Tb1—O1 | 85.19(11) |
| O7$^i$—Tb1—O4 | 79.75(11) | O6$^i$—Tb1—O4 | 124.39(11) | O1—Tb1—O4 | 139.42(11) |
| O7$^i$—Tb1—O3 | 123.92(11) | O6$^i$—Tb1—O3 | 81.55(11) | O1—Tb1—O3 | 142.83(11) |
| O4—Tb1—O3 | 74.67(11) | O7$^i$—Tb1—O1W | 73.81(12) | O6$^i$—Tb1—O1W | 140.84(12) |
| O1—Tb1—O1W | 70.94(11) | O4—Tb1—O1W | 68.83(11) | O3—Tb1—O1W | 135.42(11) |
| O7$^i$—Tb1—N1 | 146.31(13) | O6$^i$—Tb1—N1 | 140.11(13) | O1—Tb1—N1 | 93.16(12) |
| O4—Tb1—N1 | 80.65(11) | O3—Tb1—N1 | 76.00(11) | O1W—Tb1—N1 | 73.65(12) |
| O7$^i$—Tb1—N2 | 142.82(12) | O6$^i$—Tb1—N2 | 79.20(13) | O1—Tb1—N2 | 68.68(11) |
| O4—Tb1—N2 | 137.22(12) | O3—Tb1—N2 | 74.77(11) | O1W—Tb1—N2 | 117.52(12) |
| N1—Tb1—N2 | 63.37(12) | | | | |

Symmetry code: $^i$ $-x+1, -y+1, -z$.

metric unit of **1** is composed of one Tb$^{3+}$ ion, one and a half 1,4-bdc$^{2-}$ ligands, one phen ligand, and one coordinated water molecule. Tb$^{3+}$ ion is eight-coordinate and surrounded by five oxygen atoms from five 1,4-bdc$^{2-}$, one oxygen atom from the water molecule, and two nitrogen atoms from one chelating phen molecule (Fig.1a). As expected, the average distance of Tb—O (0.255 6 nm) is shorter than that of Tb—N (0.257 4 nm). 1,4-bdc$^{2-}$ adopt two kinds of coordination modes to bridge three Tb$^{3+}$ ions and four Tb$^{3+}$ ions (Fig.1b). Neighboring Tb$^{3+}$ ions are bridged by —O—C—O— links from four 1,4-bdc$^{2-}$ into a binuclear unit with Tb…Tb distance of 0.432 1 nm (Fig.1c). Such units are further bridged by 1,4-bdc$^{2-}$ into an infinite 2D plane (Fig.1d).

## 2.2 PXRD analysis and stability in organic solvents

The purity of the crystalline samples of **1** was confirmed by PXRD and the results shown in Fig.2a confirm that the PXRD pattern of the as-synthesized complex matched well with the simulated one based on the single-crystal diffraction data. To explore its stability in different solvents, crystal samples of **1** were immersed in several common organic solvents, which were ethylene glycol (EG), *N*-methyl-2-pyrrolidone (NMP), MeOH, EtOH, dimethyl sulfoxide (DMSO), *N*, *N*-dimethylformamide (DMF), *N*, *N*-dimethylacetamide (DMAC), *N*,*N*-diethylformamide (DEF), and $CH_2Cl_2$, for

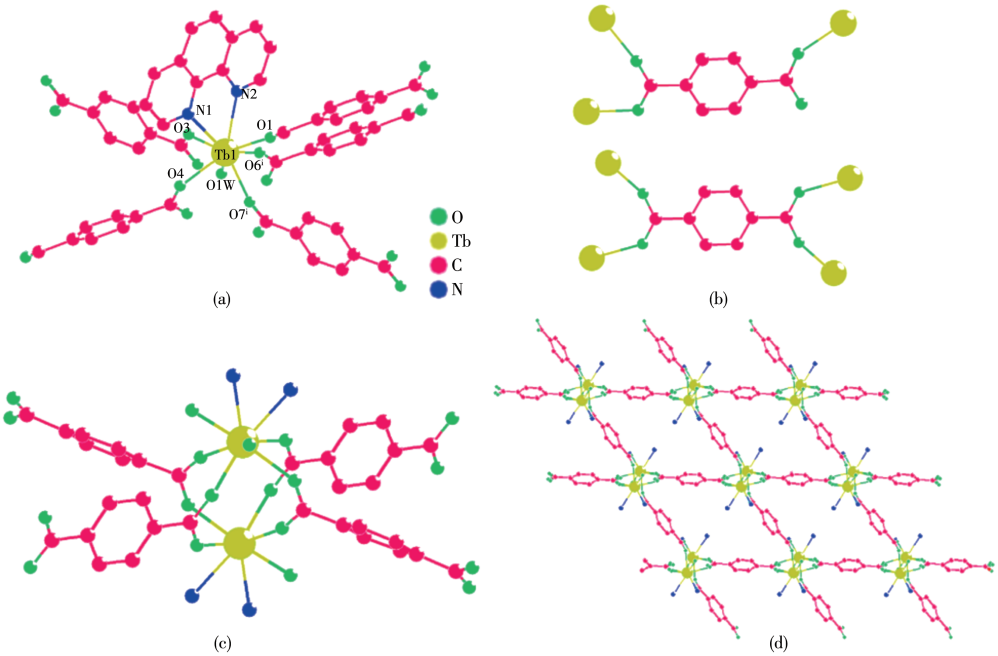


Symmetry code: $^{i}$ $-x+1, -y+1, -z$

Fig.1 Crystal structure of complex **1**: (a) coordination environment; (b) two kinds of coordination mode of 1,4-bdc$^{2-}$; (c) binuclear unit; (d) 2D plane where phen molecules are omitted for clarity

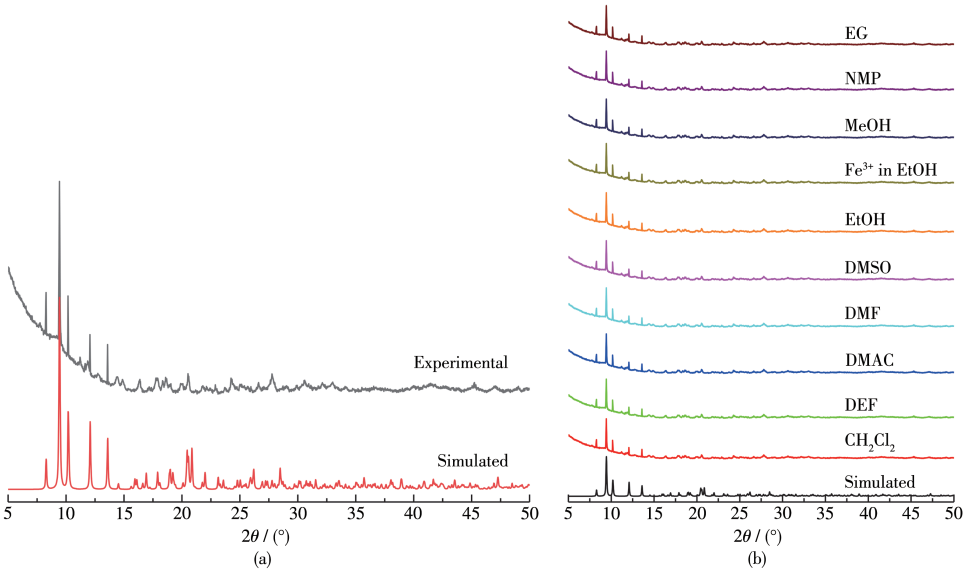


Fig.2 (a) View of simulated and experimental PXRD patterns of **1**; (b) PXRD patterns of **1** soaked in different solvents

24 h. As shown in Fig. 2b, the peak positions of the sample after soaking in different organic solvents and experimental patterns were in good agreement with each other, proving that **1** has good stability in the above organic solvents.

### 2.3 Fluorescence spectra and sensing performance

#### 2.3.1 Luminescent properties

The solid - state luminescence performance of **1** was studied at room temperature and the results are shown in Fig.3. As shown in Fig.3a, the luminescence spectrum of **1** showed a characteristic emission of Tb(Ⅲ) with an excitation wavelength of 310 nm. The emission peaks located at 489, 544, 585, 613 nm are ascribed to the $^5D_4 \rightarrow {}^7F_j$ ($j$=6, 5, 4, 3) transition of $Tb^{3+}$. To better understand its luminescent properties, the luminescence lifetime was also studied. Under 310 nm excita-

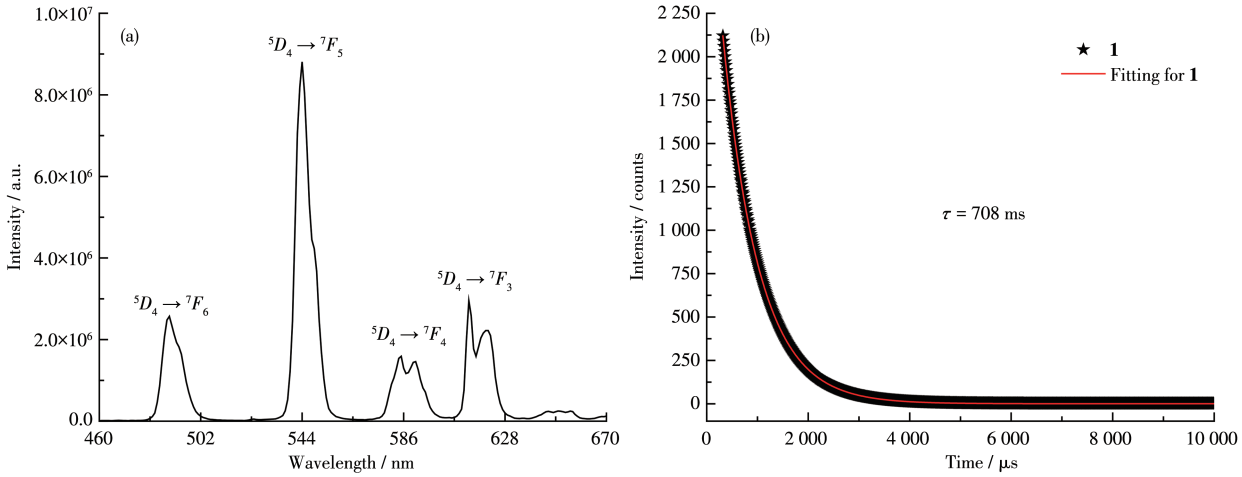


Fig.3　(a) Emission spectra of **1** in solid-state; (b) Decay curve of **1** at room temperature

tion wavelength, the luminescence lifetime was studied by monitoring the most intense peak in the whole spectrum of **1** ($^5D_4 \rightarrow {}^7F_5$). The observed luminescent lifetime determined from Fig.3b was 708 μs.

2.3.2　Sensing performance for metal ions

To investigate the sensing ability of different metal ions, the ground powder of complex **1** (3 mg) was introduced into an ethanol solution (3 mL) of $M(NO_3)_m$ ($M^{m+}$=$Ni^{2+}$, $Mn^{2+}$, $Zn^{2+}$, $K^+$, $Cd^{2+}$, $Ca^{2+}$, $Mg^{2+}$, $Fe^{3+}$, 1 mmol·L$^{-1}$). The resulting solution was homogenized under ultrasonication for 5 min, and then the fluorescence responses were recorded at room temperature (Fig.4a). The luminescence intensity at 544 nm showed a slight decrease with the addition of $Ni^{2+}$, $Mn^{2+}$, $Zn^{2+}$, $K^+$, $Cd^{2+}$, $Ca^{2+}$, and $Mg^{2+}$. On the contrary, the addition of $Fe^{3+}$ prominently decreased the luminescence intensity (almost 0), indicating that complex **1** can selectively detect $Fe^{3+}$ by fluorescence "turn-off", which also can even be observed by naked eyes (Fig.4b).

To better understand the sensitivity to $Fe^{3+}$ ions of complex **1**, a luminescence quantitative titration experiment was carried out. The luminescence intensity of complex **1** descended gradually with increasing the concentration of $Fe^{3+}$ ions (Fig. 5). Quantitatively, the calculated value of $K_{sv}$ was 8.39 × 10$^3$ L·mol$^{-1}$ using the Stern-Volmer equation at low concentration with a linear correlation coefficient value ($R^2$) of 0.995[22-26] (Fig. 6). According to LOD=3$\sigma$/$k$[27-30], the calculated

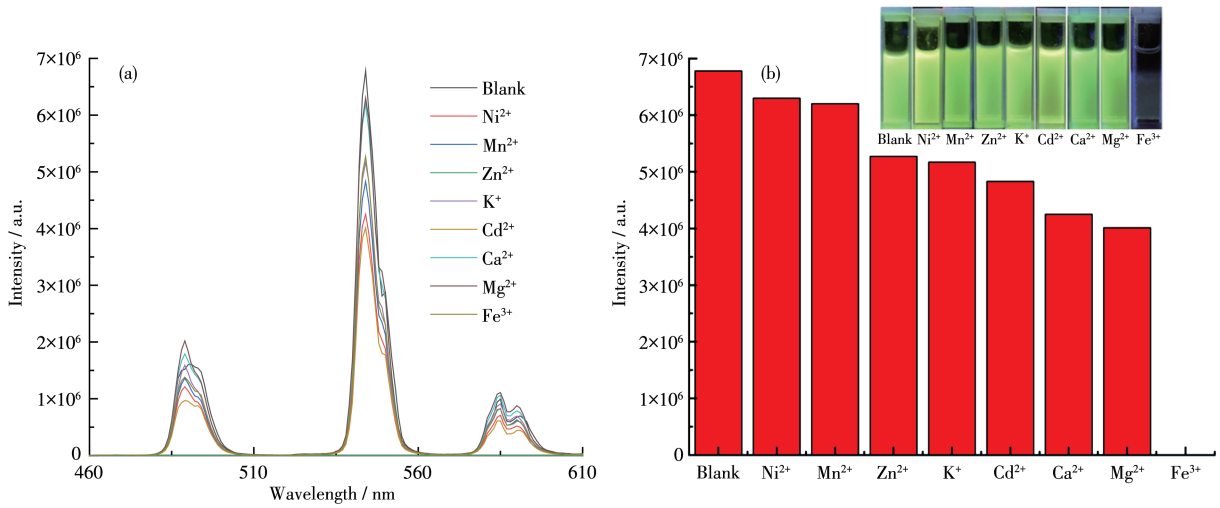


Inset: photographs of **1** under UV lamp after addition of different metal ions

Fig.4　(a) Emission spectra of **1** in ethanol solutions with different metal ions; (b) Luminescence intensity at 544 nm of **1** in different ethanol solutions of various metal ions

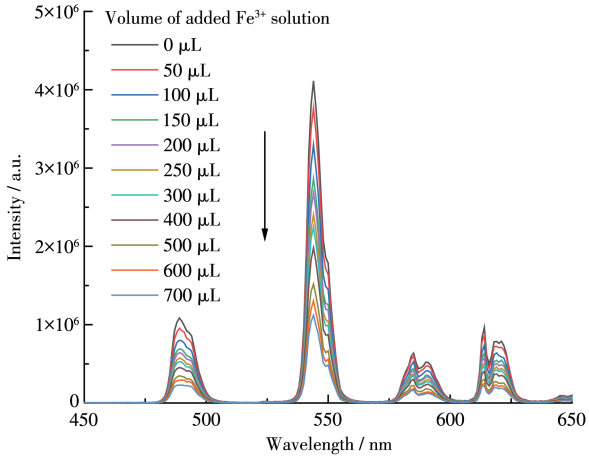


Fig.5 Emission spectra of **1** in $Fe^{3+}$ solution with various concentrations

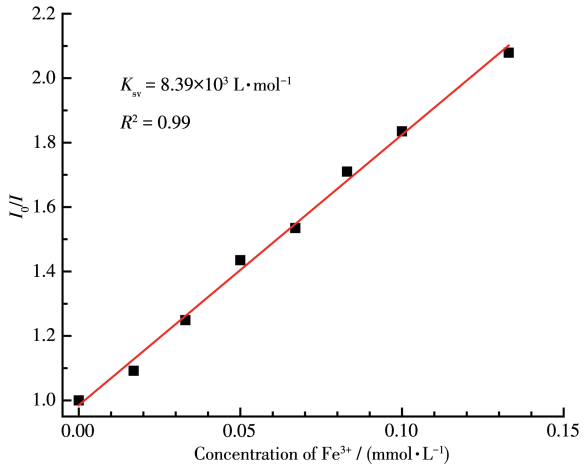


Fig.6 Stern-Volmer plot of **1** in $Fe^{3+}$ solution with various concentrations

detection limit was 0.017 μmol·$L^{-1}$. The limit of detection of compound **1** was much superior to those CPs-based sensor materials reported in the literature (Table 3).

The PXRD patterns of **1** before and after the $Fe^{3+}$ treatment proved that the crystal structure of **1** remained stable (Fig.2b), so the luminescence quenching was not caused by the decomposition of the framework. We further obtained the UV-Vis spectra of all the identified metal ions (1 mmol·$L^{-1}$ in ethanol). In Fig.7, it can be seen that the absorption band of $Fe^{3+}$ was in 300-400 nm region, which overlaps with the excitation wavelength of **1** (310 nm), indicating that there may be a competitive energy absorption progress. And other metal ions had negligible absorption on 310 nm. So, the quenching mechanism of **1** for $Fe^{3+}$ may be attributed to competitive energy absorption, which is a common quenching mechanism in CPs sensing for $Fe^{3+}$ [31-32].

Seven kinds of interference substances were used to selectively detect the identified iron ions. As shown in Fig.8, initially, with the addition of other metal ions, the fluorescence intensity of **1** showed a negligible

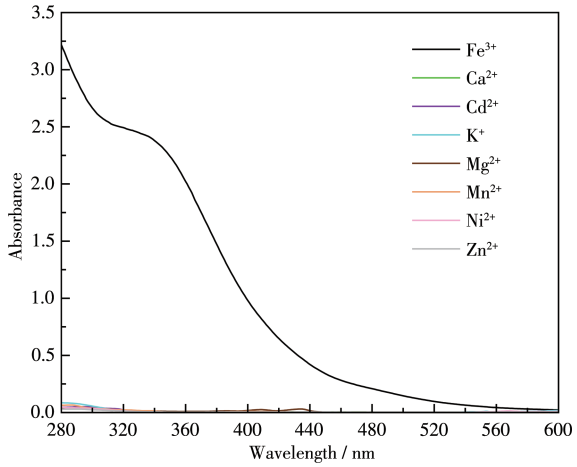


Fig.7 UV-Vis spectra of different metal ions used for the detection experiments

**Table 3 Comparison of sensing performance of compounds 1 for $Fe^{3+}$ ions with other reported CPs**

| CP | LOD / (μmol·$L^{-1}$) | $K_{sv}$ / (L·$mol^{-1}$) | Reference |
|---|---|---|---|
| $[Eu_2(L)_2(DMF)_4]_n$ | 3.69 | $1.34\times10^5$ | [22] |
| $[Tb(L)(H_2O)_3]_n$ | 1.79 | $8.39\times10^4$ | [23] |
| $\{[Tb(\mu_6\text{-}H_2cpboda)(\mu_2\text{-}OH_{2)2}]\cdot H_2O\}_n$ | 0.84 | $6.50\times10^4$ | [24] |
| Eu-MOF | 0.027 | $2.45\times10^4$ | [25] |
| Eu-BPDA | 0.9 | $1.25\times10^4$ | [26] |
| $[Eu(atpt)_{1.5}(phen)(H_2O)]_n$ | 45 | $7.60\times10^3$ | [27] |
| $[Zn(modbc)_2]_n$(Zn-CP) | 0.57 | $7.20\times10^3$ | [28] |
| 534-MOF-Tb | 0.13 | $5.51\times10^3$ | [29] |
| $[Zn_2(cptpy)(btc)(H_2O)]_n$ | 0.433 | $5.46\times10^3$ | [30] |
| $[Tb(1,4\text{-}bdc)_{1.5}(phen)(H_2O)]_n$ (**1**) | 0.017 | $8.39\times10^3$ | This work |

change (left column). However, with the addition of $Fe^{3+}$, the fluorescence intensity decreased rapidly (right column). The decrease in fluorescence intensity indicates that it can detect $Fe^{3+}$ ions even in the presence of other metal ions.

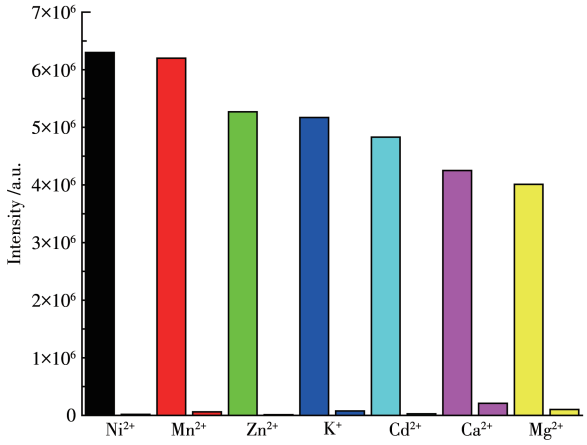


Fig.8 Fluorescence response of **1** to $Fe^{3+}$ in the presence of different ions

## 3 Conclusions

A 2D coordination polymer, [Tb(1,4-bdc)$_{1.5}$(phen)(H$_2$O)]$_n$ (**1**), was synthesized by the solvothermal method and the luminescent emission spectrum and luminescence lifetime were investigated. Compound **1** exhibited good sensitivity and selectivity for detecting $Fe^{3+}$ ions by fluorescence quenching mechanism with $K_{sv}$=8.39×10$^3$ L·mol$^{-1}$ and limit of detection of 0.017 μmol·L$^{-1}$.

## References:

[1]Chen C H, Wang X H, Li L, Huang Y B, Cao R. Highly Selective Sensing of $Fe^{3+}$ by an Anionic Metal-Organic Framework Containing Uncoordinated Nitrogen and Carboxylate Oxygen Sites. *Dalton Trans.*, **2018**,**47**:3452-3458

[2]黄佳祥,赵河,刘淑芹,张建军. 基于双核{Zn$_2$(COO)$_4$}次级构筑单元的二维发光配位聚合物的晶体结构和对Fe$^{3+}$的检测. 无机化学学报, **2021**,**37**(8):1513-1518
HUANG J X, ZHAO H, LIU S Q, ZHANG J J. Two-Dimensional Luminescent Coordination Polymer Based on Dinuclear {Zn$_2$(COO)$_4$} Second Buildings Units: Crystal Structure and Detection of $Fe^{3+}$. *Chinese J. Inorg. Chem.*, **2021**,**37**(8):1513-1518

[3]Karmakar A, Joarder B, Mallick A, Samanta P, Desai A V, Basu S, Ghosh S K. Aqueous Phase Sensing of Cyanide Ions Using a Hydrolytically Stable Metal-Organic Framework. *Chem. Commun.*, **2017**, **53**: 1253-1256

[4]Ju P, Liu X C, Zhang E S. A Novel 3D Zn-Based Luminescence Metal-organic Framework: Synthesis, Structure and Fluorescence Enhanced Sensing of Ammonia Vapor in Air. *Chin. J. Struct. Chem.*, **2020**, **39**: 1458-1464

[5]Kumar M, Li L Q, Zareba J K, Tashi L, Sahoo S C, Nyk M, Liu S J, Sheikh H N. Lanthanide Contraction in Action: Structural Variations in 13 Lanthanide(Ⅲ) Thiophene-2,5-dicarboxylate Coordination Polymers (Ln=La - Lu, Except Pm and Tm) Featuring Magnetocaloric Effect, Slow Magnetic Relaxation, and Luminescence-Lifetime-Based Thermometry. *Cryst. Growth Des.*, **2020**,**20**:6430-6452

[6]Zhao S, Hao X M, Liu J L, Wang H, Wu Y B, Guo W L. Tuning the Photoluminescence of Zn(Ⅱ) Coordination Polymers by Changing the Coordinated Solvent. *Chin. J. Struct. Chem.*, **2018**,**37**:145-151

[7]Xiao Q Q, Dong G Y, Li Y H, Cui G H. Cobalt(Ⅱ)-Based 3D Coordination Polymer with Unusual 4,4,4-Connected Topology as a Dual-Responsive Fluorescent Chemosensor for Acetylacetone and $Cr_2O_7^{2-}$. *Inorg. Chem.*, **2019**,**58**:15696-15699

[8]吴琪琪, 温一航. Tb(Ⅲ)金属有机框架材料对Cu$^{2+}$和Fe$^{3+}$的荧光检测. 无机化学学报, **2020**,**36**:941-948
WU Q Q, WEN Y H. Tb(Ⅲ)-Based Metal-Organic Framework for Simultaneously Luminescent Detection of $Cu^{2+}$ and $Fe^{3+}$ Ions. *Chinese J. Inorg. Chem.*, **2020**,**36**:941-948

[9]Yao Q X, Tian M M, Wang Y, Meng Y J, Wang J, Yao Q Y, Zhou X, Yang H, Wang H W, Li Y W, Zhang J. A Robust, Water-Stable, and Multifunctional Praseodymium-Organic Framework Showing Permanent Porosity, $CO_2$ Adsorption Properties, and Selective Sensing of $Fe^{3+}$ Ion. *Chin. J. Struct. Chem.*, **2020**,**39**:1862-1870

[10]Zhu H, Li Y H, Xiao Q Q, Cui G H. Three Luminescent Cd(Ⅱ) Coordination Polymers Containing Aromatic Dicarboxylate and Flexible Bis(benzimidazole) Ligands as Highly Sensitive and Selective Sensors for Detection of $Cr_2O_7^{2-}$ Oxoanions in Water. *Polyhedron*, **2020**, **187**:114648

[11]Zhai L J, Jiao C X, Liang J F, Zhang J, Niu X Y, Hu T P, Niu Y L. Two New Coordination Polymers Based on $H_4$BIPA-TC: Syntheses and Fluorescence Sensing for Nitroaromatic Compounds and $Fe^{3+}$ Ion. *Chin. J. Struct. Chem.*, **2020**,**39**:772-782

[12]Kong L J, Liu M, Huang H, Xu Y H, Bu X H. Metal/Covalent-Organic Framework Based Cathodes for Metal-Ion Batteries. *Adv. Energy Mater.*, **2021**:2100172

[13]陈丹丹, 衣晓虹, 王崇臣. 机械化学法制备金属-有机骨架及其复合物研究进展. 无机化学学报, **2020**,**36**(10):1805-1821
CHEN D D, YI X H, WANG C C. Preparation of Metal-Organic Frameworks and Their Composites Using Mechanochemical Methods. *Chinese J. Inorg. Chem.*, **2020**,**36**(10):1805-1821

[14]杨小青,贺春雨,张雁红,慕现贵,姜爽. 基于1,4-双(咪唑-1-基)苯的Mn(Ⅱ)/Co(Ⅱ)配位聚合物的合成、晶体结构及性质. 无机化学学报, **2021**,**37**(8):1364-1374
YANG X Q, HE C Y, ZHANG Y H, MU X G, JIANG S. Synthesis, Crystal Structure and Properties of Mn(Ⅱ)/Co(Ⅱ) Coordination Polymers Based on 1,4-Bis(imidazol-1-yl)benzene. *Chinese J. Inorg. Chem.*, **2021**,**37**(8):1364-1374

[15]Li Y. X, Han Y C, Wang C C. Fabrication Strategies and Cr(Ⅵ) Elimination Activities of the MOF-Derivatives and Their Composites. *Chem. Eng. J.*, **2021**,**405**:126648

[16]Lv X L, Feng L, Xie L H, He T, Wu W, Wang K Y, Si G R, Wang B, Li J R, Zhou H C. Linker Desymmetrization: Access to a Series of Rare-Earth Tetracarboxylate Frameworks with Eight-Connected Hexanuclear Nodes. *J. Am. Chem. Soc.*, **2021**,**143**:2784-2791

[17]Lv X L, Feng L, Wang K Y, Xie L H, He T, Wu W, Li J R, Zhou H C. A Series of Mesoporous Rare-Earth Metal-Organic Frameworks Constructed from Organic Secondary Building Units. *Angew. Chem. Int. Ed.*, **2021**,**60**:2053-2057

[18]Liu A J, Xu F, Han S D, Pan J, Wang G M. Mixed-Ligand Strategy for the Construction of Photochromic Metal-Organic Frameworks Driven by Electron-Transfer between Nonphotoactive Units. *Cryst. Growth Des.*, **2020**,**20**:7350-7355

[19]Wan Y H, Zhang L P, Jin L P, Gao S, Lu S Z. High-Dimensional Architectures from the Self-Assembly of Lanthanide Ions with Benzenedicarboxylates and 1,10-Phenanthroline. *Inorg. Chem.*, **2003**,**42**:4985-4994

[20]Wang C C, Wang X, Liu W. The Synthesis Strategies and Photocatalytic Performances of $TiO_2$/MOFs Composites: A State-of-the-Art Review. *Chem. Eng. J.*, **2020**,**391**:123601

[21]Yu M H, Liu X T, Space B, Chang Z, Bu X H. Metal-Organic Materials with Triazine-Based Ligands: From Structures to Properties and Applications. *Coord. Chem. Rev.*, **2021**,**427**:213518

[22]Xue Y S, Ding J, Sun D L, Cheng W W, Chen X R, Huang X C, Wang J. 3D Ln-MOFs as Multi-responsive Luminescent Probes for Efficient Sensing of $Fe^{3+}$, $Cr_2O_7^{2-}$, and Antibiotics in Aqueous Solution. *CrystEngComm*, **2021**,**23**:3838-3848

[23]Zhang Y X, Wu L, Feng M, Wang D M, Li C X. J. Assembly of Two-Dimension LMOF Materials with Excellent Detection of $Fe^{3+}$ Ion in Water Based on Overlap Mechanism. *Solid State Chem.*, **2021**,**294**:121868

[24]Yang D D, Lu L P, Feng S S, Zhu M L. First Ln-MOF as a Trifunctional Luminescent Probe for the Efficient Sensing of Aspartic Acid, $Fe^{3+}$ and DMSO. *Dalton Trans.*, **2020**,**49**:7514-7524

[25]Wu N, Guo H, Wang X Q, Sun L, Zhang T T, Peng L P, Yang W. A Water-Stable Lanthanide-MOF as a Highly Sensitive and Selective Luminescence Sensor for Detection of $Fe^{3+}$ and Benzaldehyde. *Colloids Surf. A*, **2021**,**616**:126093

[26]Wang J, Wang J R, Li Y, Jiang M, Zhang L W, Wu P Y. A Europium(Ⅲ)-Based Metal-Organic Framework as a Naked-Eye and Fast Response Luminescence Sensor for Acetone and Ferric Iron. *New J. Chem.*, **2016**,**40**:8600-8606

[27]Kang Y X, Zheng J, Jin L P. A Microscale Multi-Functional Metal-Organic Framework as a Fluorescence Chemosensor for Fe(Ⅲ), Al(Ⅲ) and 2-Hydroxy-1-naphthaldehyde. *J. Colloid Interface Sci.*, **2016**,**471**:1-6

[28]Wu Y, Liu D, Lin M, Qian J. Zinc(Ⅱ)-Based Coordination Polymer Encapsulated $Tb^{3+}$ as a Multi-Responsive Luminescent Sensor for $Ru^{3+}$, $Fe^{3+}$, $CrO_4^{2-}$, $Cr_2O_7^{2-}$ and $MnO_4^-$. *RSC Adv.*, **2020**,**10**:6022-6029

[29]Chen M, Xu W M, Tian J Y, Cui H, Zhang J X, Liu C S, Du M. A Terbium(Ⅲ) Lanthanide-Organic Framework as a Platform for a Recyclable Multi-Responsive Luminescent Sensor. *J. Mater. Chem. C*, **2017**,**5**:2015-2021

[30]Chen H J, Fan P, Tu X X, Min H, Yu X Y, Li X F, Zeng J L, Zhang S W, Cheng P. A Bifunctional Luminescent Metal-Organic Framework for the Sensing of Paraquat and $Fe^{3+}$ Ions in Water. *Chem. Asian J.*, **2019**,**14**:3611-3619

[31]Qu T G, Hao X M, Wang H, Cui X G, Chen F, Wu Y B, Yang D, Zhang M, Guo W L. A Luminescent 2D Zinc(Ⅱ) Metal-Organic Framework for Selective Sensing of Fe(Ⅲ) Ions and Adsorption of Organic Dyes. *Polyhedron*, **2018**,**156**:208-217

[32]Yin J C, Li N, Qian B B, Yu M H, Chang Z, Bu X H. Highly Stable Zn-MOF with Lewis Basic Nitrogen Sites for Selective Sensing of $Fe^{3+}$ and $Cr_2O_7^{2-}$ Ions in Aqueous Systems. *J. Coord. Chem.*, **2020**,**73**:2718-2727